

# Half-metallicity at the (110) interface between a full Heusler alloy and GaAs

Kazutaka Nagao, Yoshio Miura, and Masafumi Shirai

Research Institute of Electrical Communication, Tohoku University, 2-1-1 Katahira, Aoba-ku, Sendai 980-8577, Japan

(Received 12 September 2005; revised manuscript received 19 January 2006; published 29 March 2006)

The electronic properties of  $\text{Co}_2\text{CrAl}/\text{GaAs}$  interfaces are investigated by using first-principles calculations with density functional theory. It is found that spin polarization tends to remain relatively high at the (110) interface and reaches almost unity for a specific (110) interfacial structure. Furthermore, the nearly-half-metallic interface turns out to be the most stable of the (110) interfacial structures studied here. Spin polarization calculated only from the  $sp$ -projected density of states is also examined in order to eliminate the effects stemming from the localized  $d$  components. The analysis shows that the high spin polarization at the (110) interface owes little to the localized  $d$  component and, therefore, is expected to be fairly relevant to transport properties.  $\text{Co}_2\text{CrSi}/\text{GaAs}$ ,  $\text{Co}_2\text{MnSi}/\text{GaAs}$ , and  $\text{Co}_2\text{MnGe}/\text{GaAs}$  heterostructures are also investigated, and similar half-metal-like behavior at (110) interface is observed for all of them.

DOI: [10.1103/PhysRevB.73.104447](https://doi.org/10.1103/PhysRevB.73.104447)

PACS number(s): 75.70.-i, 73.20.-r, 85.75.-d

## I. INTRODUCTION

The half-metallic ferromagnet, which is metallic for one of spin-up and spin-down states and semiconducting for the other, has long been expected well to work as a spin filter or spin-injecting source capable of generating extremely spin-polarized current. Since de Groot *et al.* first predicted that  $\text{NiMnSb}$  possesses half-metallic character,<sup>1</sup> so far many substances have been proposed as half metal from first-principles calculations.<sup>2–8</sup> However, intriguingly, most of the half metals have not fully exhibited their unique character (i.e., complete spin polarization at the Fermi energy) when they are incorporated into heterostructures constructed for the purpose of attaining, e.g., a high tunneling magnetoresistance (TMR) ratio or efficient spin injection into semiconductors. Recently, using  $\text{La}_{2/3}\text{Sr}_{1/3}\text{MnO}_3/\text{SrTiO}_3/\text{La}_{2/3}\text{Sr}_{1/3}\text{MnO}_3$  magnetic tunnel junction, Bowen *et al.*<sup>9</sup> successfully observed a TMR ratio of  $\sim 1800\%$ , which corresponds to the spin polarization of  $\sim 95\%$  according to Jullière's model.<sup>10</sup> Yet confirmation of such a high spin polarization is quite rare, even at low temperatures. One of the causes of the reduced performance of half metals might be the deterioration of half-metallicity in the vicinity of the boundary with other substances. The interfacial properties of half metals have so far been investigated in detail by first-principles calculations,<sup>11–13</sup> and it is known that half metals almost always lose the completely spin-polarized character at interfaces. Exceptional half-metallic interfaces are theoretically found only for a few cases: for example,  $\text{NiMnSb}/\text{CdS}$  (Ref. 14) and zinc-blende  $\text{CrAs}/\text{GaAs}$  (Refs. 15 and 16) interfaces. It is still unclear and controversial how much the interfacial electronic structures affect the spin polarization of current. However, at least as long as the functioning of devices relies on coherent tunneling, their performance seems to be sensitive to the condition of interface.<sup>17–19</sup>

In this paper, we chiefly investigate the interfacial properties of  $\text{Co}_2\text{CrAl}/\text{GaAs}$  heterostructures using first-principles calculations, where we focus our attention on (100) and (110) interfaces.<sup>20</sup>  $\text{Co}_2\text{CrAl}$  is one of the full Heusler alloys that have been predicted to possess half-metallic electronic structures, and its Curie temperature is higher than room

temperature ( $T_c \sim 334$  K).<sup>21</sup> It is also known from first-principles calculations that the half-metallicity is robust against Cr-Al substitutional disorder, which is likely to occur in real systems.<sup>22</sup> Recently, a substance similar to  $\text{Co}_2\text{CrAl}$ —namely,  $\text{Co}_2(\text{Fe}, \text{Cr})\text{Al}$  (Refs. 22–24) was utilized for TMR devices, and a TMR ratio of 19% was achieved at room temperature.<sup>25,26</sup> In what follows, we show that this half-metallic  $\text{Co}_2\text{CrAl}$  still keeps its high spin polarization even at interfaces when it makes heterojunctions with GaAs along the [110] orientation. This finding suggests the possibilities both of gaining a high TMR ratio with low resistance (compared with oxide tunneling barriers) and of achieving efficient spin injection into semiconductors by the use of  $\text{Co}_2\text{CrAl}/\text{GaAs}$  heterojunctions. Besides  $\text{Co}_2\text{CrAl}$ , we also examine other full Heusler alloys  $\text{Co}_2\text{CrSi}$ ,  $\text{Co}_2\text{MnSi}$ , and  $\text{Co}_2\text{MnGe}$ , which are half metallic in the bulk state, and briefly discuss their electronic structures at the interface with GaAs in comparison with the  $\text{Co}_2\text{CrAl}/\text{GaAs}$  interface.

## II. TECHNICAL DETAILS

We perform first-principles calculations for multilayers consisting of  $\text{Co}_2\text{CrAl}$  and GaAs, using density functional theory within generalized gradient approximation (GGA).<sup>27</sup> In order to facilitate the optimization of atomic coordinates, which is crucial for investigating interfacial properties, we make use of plane-wave basis sets together with the projector augmented-wave (PAW) method.<sup>28,29</sup> Throughout this paper, we utilize the Vienna *ab initio* simulation program<sup>30–32</sup> to implement these calculations.

A  $\text{Co}_2\text{CrAl}/\text{GaAs}$  multilayer is constructed in a supercell, where the two interfaces within a supercell are made to possess the same interfacial structure. The slabs of  $\text{Co}_2\text{CrAl}$  and GaAs are, respectively, composed of 11 and 13 atomic layers for the (100) interface and of 8 and 10 atomic layers for the (110) interface. These thicknesses are large enough to reproduce the bulk properties of both  $\text{Co}_2\text{CrAl}$  and GaAs around the middle of the slabs. The in-plane lattice parameters of the supercell,  $a$  and  $b$ , are chosen to be in accordance with those of bulk GaAs; more specifically,  $(a, b)$  are  $(a_{\text{GaAs}}/\sqrt{2},$

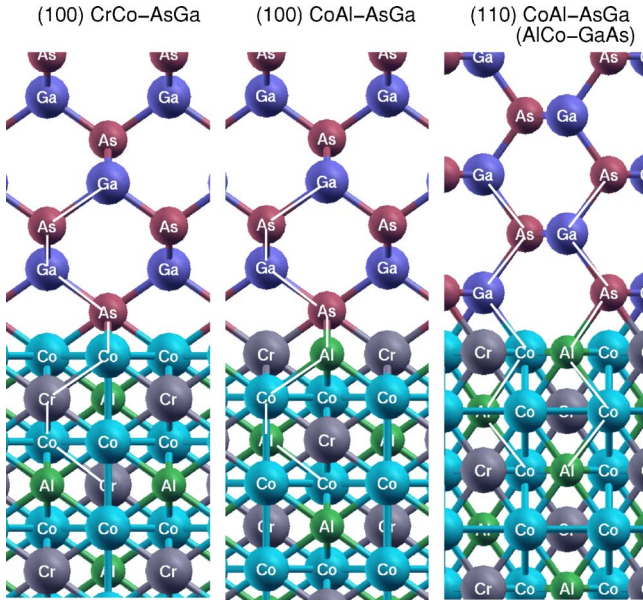


FIG. 1. (Color online) Examples of the interfacial structures studied in this paper. The white solid line is drawn to help find out the path where zinc-blende structures are connected (see text).

$a_{\text{GaAs}}/\sqrt{2}$ ) for the (100) interface and  $(a_{\text{GaAs}}/\sqrt{2}, a_{\text{GaAs}})$  for the (110) interface, where  $a_{\text{GaAs}}$  is set to a value known from experiments: namely, 5.65 Å. On the other hand, the lattice parameter along the direction perpendicular to the interface  $c$  is optimized for both (100) and (110) interfaces. The atomic coordinates are fully relaxed from initial atomic configurations. The number of  $\mathbf{k}$  points is taken to be  $10 \times 10 \times 1$  for the (100) interface and  $10 \times 7 \times 1$  for the (110) interface,<sup>33</sup> and a Fermi-distribution smearing with the temperature of  $k_B T = 0.1$  eV is used. The cutoff energy is set to  $\sim 290$  eV, which is large enough to deal with all the elements considered here within the PAW method. The outermost cutoff radii of each pseudopotential are taken to be 1.22 Å for Co, 1.32 Å for Cr, 0.90 Å for Al, 1.22 Å for Ga, and 1.11 Å for As, where  $3d$  states are treated as core states only for the As atom. For the computation of the local density of states (LDOS), the sphere sizes of each atom are set to 1.26 Å for Co, 1.27 Å for Cr, 1.18 Å for Al, 1.26 Å for Ga, and 1.19 Å for As, and the smearing width is set to 0.05 eV.

Upon choosing the initial condition of the interfacial structure, we pay attention to the fact that  $\text{Co}_2\text{CrAl}$  can be seen as composed of two zinc-blende (ZB) structures (i.e., ZB-CoCr and ZB-CoAl), one of which is located on the vacancy sites of the other. Thus, as initial atomic configurations, we take the interfacial structures where one of the ZB-CoCr and ZB-CoAl inside  $\text{Co}_2\text{CrAl}$  is connected to the ZB structure of GaAs. A few examples of the structures are illustrated in Fig. 1. Here, we call each structure by referring to the atoms on the path where ZB structures are connected; e.g., “(100) CrCo-AsGa” (left panel) means that ZB-CoCr inside  $\text{Co}_2\text{CrAl}$  is connected to ZB-GaAs at the (100) interface and also that the Co and As atoms are neighbored there. Notice that for the (110) interfaces, there are two ways of denoting each structure. For example, “(110) CoAl-AsGa” and “(110) AlCo-GaAs” designate the same structure (right

panel), and we therefore use one of them as its label.

All the details mentioned above are kept throughout the paper unless otherwise stated. Also, the same computational conditions are applied to the other Heusler alloys: namely,  $\text{Co}_2\text{CrSi}$ ,  $\text{Co}_2\text{MnSi}$ , and  $\text{Co}_2\text{MnGe}$ . Regarding Si, Mn, and Ge elements, the outermost cutoff radii of pseudopotentials are 1.01 Å for Si, 1.22 Å for Mn, and 1.22 Å for Ge, and the sphere sizes for calculating LDOS are 1.11 Å for Si, 1.39 Å for Mn, and 1.22 Å for Ge.

### III. RESULTS

For the interfaces constructed as above, we first investigate the spin polarization of atoms defined from the LDOS: namely,

$$P = \frac{D_{\uparrow}(\epsilon_F) - D_{\downarrow}(\epsilon_F)}{D_{\uparrow}(\epsilon_F) + D_{\downarrow}(\epsilon_F)},$$

where  $D_{\uparrow}(\epsilon_F)$  and  $D_{\downarrow}(\epsilon_F)$  are the LDOS of each atom at the Fermi energy for up and down spins, respectively. The resulting spin polarization of Co, Cr, and Al atoms located at the interface (and at the free surface for comparison) is presented in Table I, where the magnetic moment of the atoms is also shown.

In most cases the half-metallicity is deteriorated at the interface, but the spin polarization tends to remain relatively high at the (110) interfaces as a whole. In particular, there exist two (110) interfacial structures where extremely high spin polarization is retained. Those are the (110) CoAl-AsGa and (110) CoCr-AsGa structures, and the half-metal-like property is more complete in the former. Notice that these two interfacial structures interchange by exchanging the positions of the Cr and Al atoms. The high spin polarization at both the interfaces hence implies that the nearly-half-metallic character is robust against Cr-Al substitutional disorder.<sup>22</sup> In fact, the high spin polarization is well preserved at least with respect to the exchange of the Cr and Al atoms on the interfacial layer for the (110) CoAl-AsGa and (110) CoCr-AsGa cases.

Spin polarization is also found to remain rather high at the (100) interface when  $\text{Co}_2\text{CrAl}$  has a CrAl-terminated internal surface. Especially, the (100) CoAl-AsGa interface gives rise to high spin polarization. The spin polarization, however, looks a little deviated from unity when compared with that of the nearly-half-metallic (110) cases. It is worth mentioning that the (100) CrAl-terminated *surface* was previously predicted to have half-metallic character.<sup>34</sup> The half-metallic property at the CrAl-terminated surface is, however, lost once the surface is attached to GaAs. Indeed, a significant change of electronic structures from the surface to interface is observed in the magnetic moment. The difference in magnetic moment between the surface and interface is more prominent for one of the Co atoms on the second layer from the interface than for the Cr atom on the interfacial layer. The Co atom is, in fact, somewhat close to the Ga or As atom on the GaAs internal surface (the distance is  $\sim 3.3$  Å) since the Co atom is located on the position which corresponds to the *neighboring vacancy site* of the Ga or As atom. This structural feature is peculiar to the (100) interface, and the same

TABLE I. Local spin polarization  $P$  and magnetic moment  $\mu$  in units of the Bohr magneton  $\mu_B$  at the  $\text{Co}_2\text{CrAl}/\text{GaAs}$  interface and at the  $\text{Co}_2\text{CrAl}$  surface. Spin polarization of the atoms which are on the second atomic layer from the interface (or from the surface) is shown with an asterisk. See the text and Fig. 1 for the way of denoting the interfacial structure.

Orientation and structural type		$P$			$\mu/\mu_B$				
		Co	Cr	Al	Co	Cr	Al		
(100)	Co-terminated surface	0.11	0.11	*0.69	*0.55	0.71	0.71	*0.46	*-0.03
	CrCo-GaAs	0.30	0.50	*0.91	*0.45	-0.32	0.41	*0.91	*-0.03
	CrCo-AsGa	0.57	0.50	*0.97	*0.65	0.05	0.51	*1.31	*-0.04
	AlCo-GaAs	0.21	0.12	*0.90	*0.41	-0.27	0.68	*0.77	*-0.03
	AlCo-AsGa	0.56	0.30	*0.95	*0.70	0.13	0.69	*1.17	*-0.04
(100)	CrAl-terminated surface	*0.96	*0.96	0.97	0.74	*0.76	*0.76	2.84	-0.02
	CoCr-GaAs	*0.55	*0.75	0.63	-0.09	*0.39	*0.72	2.64	-0.04
	CoCr-AsGa	*0.69	*0.85	0.81	-0.05	*0.32	*0.71	2.53	-0.04
	CoAl-GaAs	*0.60	*0.83	0.81	0.45	*0.46	*0.61	2.62	-0.05
	CoAl-AsGa	*0.83	*0.93	0.94	0.76	*0.29	*0.70	2.50	-0.03
(110)	surface	0.47	0.47	0.65	0.45	-0.61	-0.61	1.98	-0.02
	CoCr-GaAs (CrCo-AsGa)	0.32	0.80	0.92	0.67	1.12	-0.06	1.85	-0.03
	CoCr-AsGa (CrCo-GaAs)	0.71	0.99	0.99	0.95	1.15	-0.20	1.64	-0.03
	CoAl-GaAs (AlCo-AsGa)	0.35	0.77	0.91	0.70	0.95	0.35	1.84	-0.04
	CoAl-AsGa (AlCo-GaAs)	0.89	0.99	1.00	0.97	1.14	0.02	1.75	-0.03

effect on the second layer is also found for the (100) interfaces with Co-terminated internal surface.

At this point, we check the sensitivity of the half-metal-like property at the (110) interface to the choice of lattice parameters because the GGA and the local density approximation (LDA) lead to slightly different GaAs lattice constants:  $a_{\text{GaAs}}=5.74 \text{ \AA}$  in the GGA and  $a_{\text{GaAs}}=5.61 \text{ \AA}$  in the LDA. We therefore carry out similar calculations using the in-plane lattice parameters  $(a, b)=(a_{\text{GaAs}}/\sqrt{2}, a_{\text{GaAs}})$  with  $a_{\text{GaAs}}=5.74 \text{ \AA}$  and  $a_{\text{GaAs}}=5.61 \text{ \AA}$ . Here, the lattice parameter  $c$  is unchanged from the optimized value used so far. We use the GGA in these calculations because the LDA is not considered suitable for treating  $\text{Co}_2\text{CrAl}$ . The results show that the half-metal-like property at the (110) interface is almost unaffected by these changes of lattice parameters. In the (110) CoAl-AsGa case, spin polarization is increased for  $a_{\text{GaAs}}=5.61 \text{ \AA}$  and decreased for  $a_{\text{GaAs}}=5.74 \text{ \AA}$ , and the decrease is less than 0.03. In the (110) CoCr-AsGa case, likewise, spin polarization is decreased only for  $a_{\text{GaAs}}=5.74 \text{ \AA}$ , and the decrease is less than 0.01. The increase of spin polarization for  $a_{\text{GaAs}}=5.61 \text{ \AA}$  originates in the properties of *bulk*  $\text{Co}_2\text{CrAl}$ , where the reduction of volume has an effect to enlarge the minority-spin gap.

Now we investigate the electronic properties in a little more detail choosing the interfacial structures which have the highest spin polarization in each termination type of  $\text{Co}_2\text{CrAl}$ : namely, the (100) CrCo-AsGa, (100) CoAl-AsGa, and (110) CoAl-AsGa interfaces. Figure 2 shows the spatial behavior of local spin polarization of the three interfaces. Spin polarization is almost unity around the middle of  $\text{Co}_2\text{CrAl}$  slab (around  $z \sim -7.5 \text{ \AA}$ ) in all cases, and this confirms that the thickness of the slab is large enough to recover the bulk properties of  $\text{Co}_2\text{CrAl}$ . A significant decrease of spin

polarization at the interface is observed only in the (100) CrCo-AsGa interface [Fig. 2(a)]. The retrieval of the deteriorated spin polarization is, however, found very quick for Cr atoms. Actually, the spin polarization of Cr atoms almost reaches unity on the second atomic layer from the interface

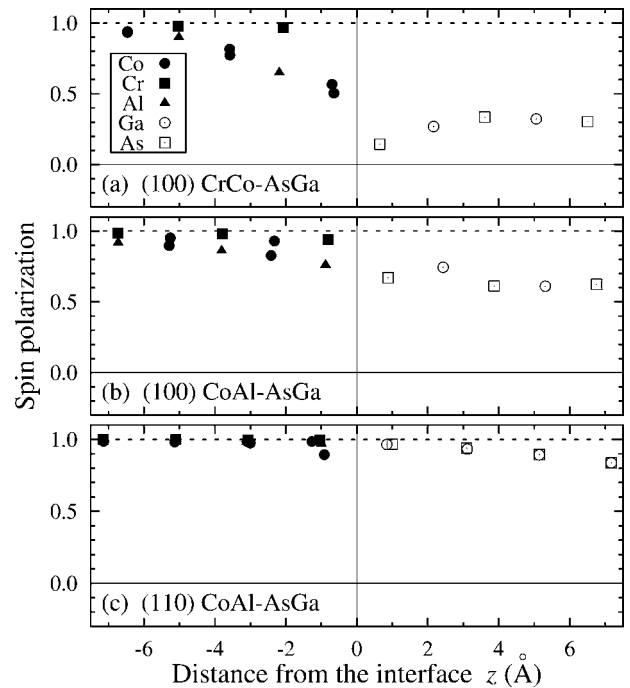


FIG. 2. Local spin polarization as a function of the distance from the  $\text{Co}_2\text{CrAl}/\text{GaAs}$  interface, where the interfacial structures are set to (100) CrCo-AsGa (a), (100) CoAl-AsGa (b), and (110) CoAl-AsGa (c).

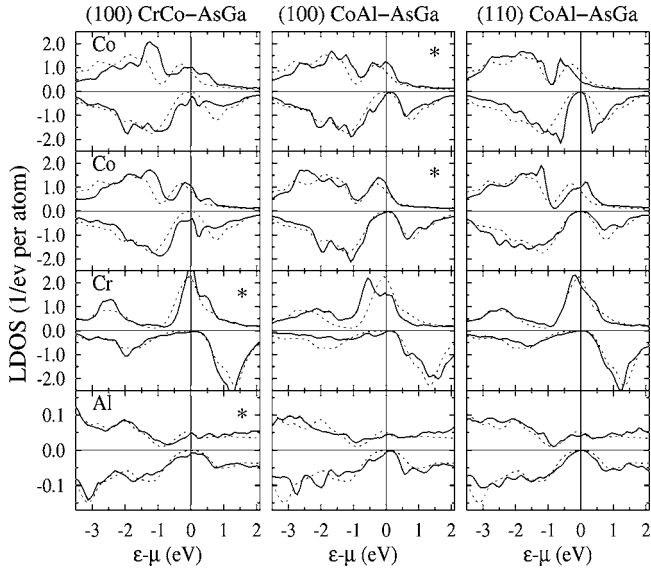


FIG. 3. LDOS at the  $\text{Co}_2\text{CrAl}/\text{GaAs}$  interface, where the interfacial structures are set to (100) CrCo-AsGa (left panel), (100) CoAl-AsGa (middle panel), and (110) CoAl-AsGa (right panel). The minority-spin LDOS is shown with a negative sign. For comparison, the bulk LDOS is also presented as a dashed line. Asterisks denote that the atoms are located on the second atomic layer from the interface.

(at  $z \sim -2 \text{ \AA}$ ) while those of Co and Al atoms require about three-atomic-layer thickness completely to recover. Similar behavior is also found in the (100) CoAl-AsGa interface [Fig 2(b)] though the deviation of spin polarization from unity is smaller. Although spin polarization is not well defined in bulk semiconductors, it is here calculated inside the GaAs slab because gap states are induced in the region close to the interface.<sup>11</sup> It is impressive that for the (110) CoAl-AsGa interface [Fig. 2(c)], the spin polarization remains very high inside GaAs. The size of spin polarization inside GaAs seems to be relevant to that at the internal surface of  $\text{Co}_2\text{CrAl}$  and does *not* sensitively change as a function of the distance from the interface for all three cases. This behavior is in accordance with the observation that the decay length of the gap states is rather independent of their origins and is therefore of similar size for both up and down spins.<sup>11,35</sup>

Figure 3 presents the LDOS at the interface, where the bulk LDOS is also shown for comparison. In the (110) CoAl-AsGa case (right panel), a dip is found in the minority-spin LDOS at the Fermi energy. Its width is smaller than that in the bulk state, yet the dip still keeps its shape clearly and the depletion is almost complete in the vicinity of the Fermi energy. In contrast, in the (100) CoAl-AsGa case (middle panel) where the spin polarization itself results in being relatively high as seen in Fig. 2(b), a small accumulation of minority-spin states is observed just below the Fermi energy. This suggests that the spin polarization may be easily decreased by such external conditions as temperature, resulting thermal expansion, etc. In the (100) CrCo-AsGa case (left panel), the majority-spin LDOS of the Cr atom has a sharp peak at the Fermi energy; the peak leads to a high Cr spin polarization in spite of the appearance of minority-spin states around the Fermi energy. The sharp peak, however, means

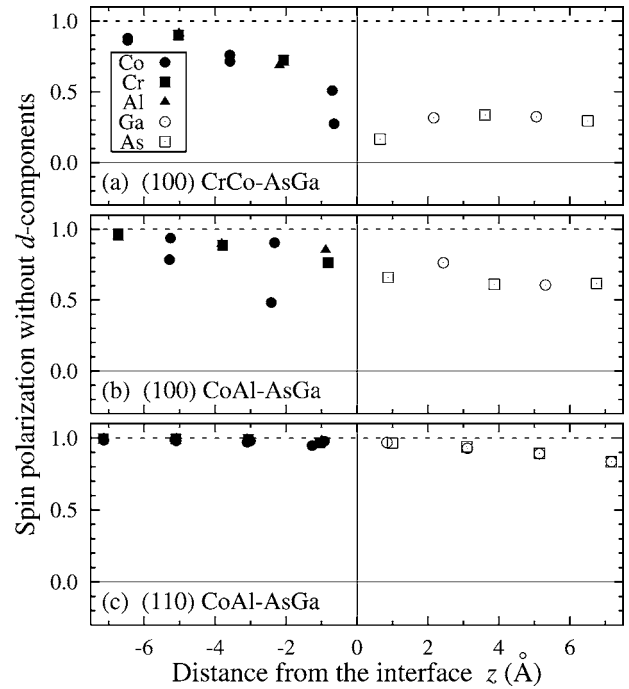


FIG. 4. Local spin polarization estimated from the LDOS without  $d$  components as a function of the distance from the  $\text{Co}_2\text{CrAl}/\text{GaAs}$  interface, where the interfacial structures are set to (100) CrCo-AsGa (a), (100) CoAl-AsGa (b), and (110) CoAl-AsGa (c).

that the states contributing to the high spin polarization are largely composed of localized  $d$  components. Accordingly, the rapid recovery of the Cr spin polarization shown in Fig. 2(a) may have little relevance to the spin polarization of *current*.

One conceivable way to avoid the influence of localized states is, for example, to investigate the Fermi velocities.<sup>36</sup> However, if the Fermi velocities are calculated for the supercells used in this study, they must be regarded as the *bulk* properties possessed by  $\text{Co}_2\text{CrAl}/\text{GaAs}$  *multilayers*, which have quite different boundary conditions from those of magnetic junctions, etc. Hence, in this paper, we rather choose to inspect the quantity which is fairly insensitive to boundary conditions and yet reasonably relevant to transport properties: namely, the spin polarization defined from the LDOS without  $d$  components.

The results are shown in Fig. 4. As anticipated, in the (100) CrCo-AsGa case [Fig. 4(a)], the spin polarization of the Cr atom is lowered a lot. This tendency is similarly observed in the (100) CoAl-AsGa interface [Fig. 4(b)], where the spin polarization of the Co atom on the second layer is significantly decreased. For both of these two (100) interfaces, the recovery of spin polarization inside  $\text{Co}_2\text{CrAl}$  turns out to be slowed: It takes four or five atomic layers for the decreased spin polarization to reach its bulk value. In the (110) CoAl-AsGa interface [Fig. 4(c)], the behavior of spin polarization is in marked contrast to those in the (100) interfaces. The high spin polarization seen in Fig. 4(c) is almost unaffected or even looks slightly enhanced by the elimination of the  $d$  components. The nearly-half-metallic character

TABLE II. Adhesion energy  $W$  (ideal work of separation) of  $\text{Co}_2\text{CrAl}/\text{GaAs}$  interfaces.

Orientation and structural type		$W$ (J/m <sup>2</sup> )
(100)	AlCo-AsGa	2.95
	CrCo-AsGa	2.74
	AlCo-GaAs	2.72
	CrCo-GaAs	2.60
	CoCr-AsGa	1.93
	CoAl-AsGa	1.71
	CoAl-GaAs	1.66
	CoCr-GaAs	1.42
(110)	CoAl-AsGa (AlCo-GaAs)	1.76
	CoAl-GaAs (AlCo-AsGa)	1.69
	CoCr-AsGa (CrCo-GaAs)	1.64
	CoCr-GaAs (CrCo-AsGa)	1.34

at (110) interface is, therefore, thought to be highly related to the transport properties.

We then inquire into the adhesion energy  $W$  to assess the strength of the interfaces. Here, the adhesion energy is defined as the ideal work of separation and is calculated from<sup>37,38</sup>

$$W = (E_{\text{CCA}} + E_{\text{GA}} - E_{\text{CCA/GA}})/2A,$$

where  $E_{\text{CCA}}$ ,  $E_{\text{GA}}$ , and  $E_{\text{CCA/GA}}$  are the energies of an isolated  $\text{Co}_2\text{CrAl}$  slab, isolated GaAs slab, and  $\text{Co}_2\text{CrAl}/\text{GaAs}$  multilayer within a supercell, respectively, and  $A$  is the area of the interface. The factor of 2 in the denominator is in order to take account of the existence of the two interfaces in the supercell. The calculated adhesion energy is listed in Table II. The (100) CoAl-AsGa, which has relatively high spin polarization, does not have the strongest adhesion of the (100) interfaces. This structure thus seems to be less probable as a (100) interface. Remarkably, the (110) CoAl-AsGa, which is nearly half-metallic, has the strongest adhesion of the (110) interfaces. It should be noticed that all four (110) interfacial structures contain the same number of atoms with the same chemical composition in the supercell. Thus, as long as the (110) interface is concerned, the largest adhesion energy simultaneously means the lowest interface energy. The nearly-half-metallic (110) CoAl-AsGa interface is therefore considered the most stable both mechanically and energetically in the (110) interfaces.

It is interesting to note that the electronic structure at the (110) *surface* of  $\text{Co}_2\text{CrAl}$  is far from half metallic (see Table I). This implies that the nearly-half-metallic character at the (110) interface owes a lot to the properties of the GaAs (110) plane. Figure 5 shows the LDOS of GaAs at the nearly-half-metallic interface, where unrelaxed and relaxed (110) CoAl-AsGa interfaces are considered. Even at the interface where the atomic relaxation is not taken account of (left panel), a clear dip in the minority-spin LDOS is observed at the Fermi energy. The dip predominantly stems from the fact that the (110) plane has two kinds of atomic positions (i.e., Ga and As sites) and, therefore, the localized states which are

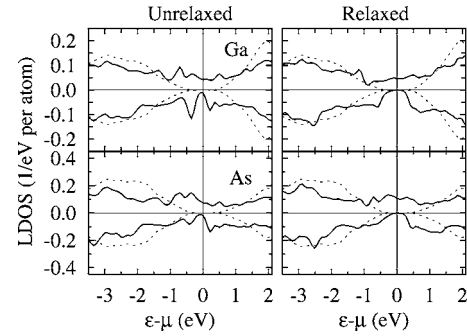


FIG. 5. LDOS of GaAs at the  $\text{Co}_2\text{CrAl}/\text{GaAs}$  interface, where the interfacial structure is set to (110) CoAl-AsGa. In the left panel, the atomic coordinates are not relaxed, but the interlayer distance at the interface is optimized; this optimization results in a lattice parameter  $c$  of 36.4 Å. In the right panel, the atomic coordinates are relaxed while  $c$  is kept at 36.4 Å. For comparison, the bulk LDOS is also presented as a dashed line.

near the Fermi energy are split. Furthermore, as seen in the right panel of Fig. 5, the relaxation of the atomic position significantly widens the dip and enhances the minority-spin gap. It should be noted that similar behavior is also found at the GaAs (110) *surface*. Indeed, the GaAs (110) surface evades the appearance of localized states at the Fermi energy just by making a structural reconstruction within the  $1 \times 1$  periodicity,<sup>39</sup> while the GaAs (100) surface needs extensive and complicated surface reconstruction for reducing the number of dangling bonds.<sup>40</sup> Regarding the majority-spin states, for which  $\text{Co}_2\text{CrAl}$  is metallic, the delocalized wave functions of  $\text{Co}_2\text{CrAl}$  penetrate into GaAs, giving rise to metal-induced gap states.<sup>41</sup> Consequently, there are found appreciable majority-spin LDOS at the Fermi energy even inside GaAs around the interface. This scenario is applicable to all (110) interfacial structures, but it is occasionally disturbed by other factors. Actually, two out of the four (110) interfaces studied in this paper lose half-metallicity as shown in Table I. The loss of half-metallicity in the two cases—namely, the (110) CoAl-GaAs and (110) CoCr-GaAs cases—is attributed to the reaction between Co and As atoms. The initial positions of the Co and As atoms are very close in these two interfacial structures, and this structural property leads to appreciable Co-As bonding, resulting in a decreased spin polarization.

If the high spin polarization at the (110) interface largely comes from the properties of the GaAs (110) plane as suggested above, a similar tendency should also be expected for other half metals. This speculation prompts us to make an inspection of the interfacial properties with regard to other full Heusler alloys. Thus, choosing  $\text{Co}_2\text{CrSi}$ ,  $\text{Co}_2\text{MnSi}$ , and  $\text{Co}_2\text{MnGe}$ , which are likewise half-metallic in the bulk state, we carry out the same calculations for them as those for  $\text{Co}_2\text{CrAl}$ .

The LDOS at  $\text{Co}_2YZ/\text{GaAs}$  ( $YZ = \text{CrSi}$ ,  $\text{MnSi}$ , and  $\text{MnGe}$ ) interfaces are shown in Fig. 6, where the interfacial structures are taken to be (110) CoZ-AsGa. Interestingly, a clear dip at the Fermi energy is found in minority-spin LDOS for all the three alloys (though the half-metal-like behavior is less complete for  $\text{Co}_2\text{CrSi}/\text{GaAs}$  and  $\text{Co}_2\text{MnGe}/\text{GaAs}$ ,

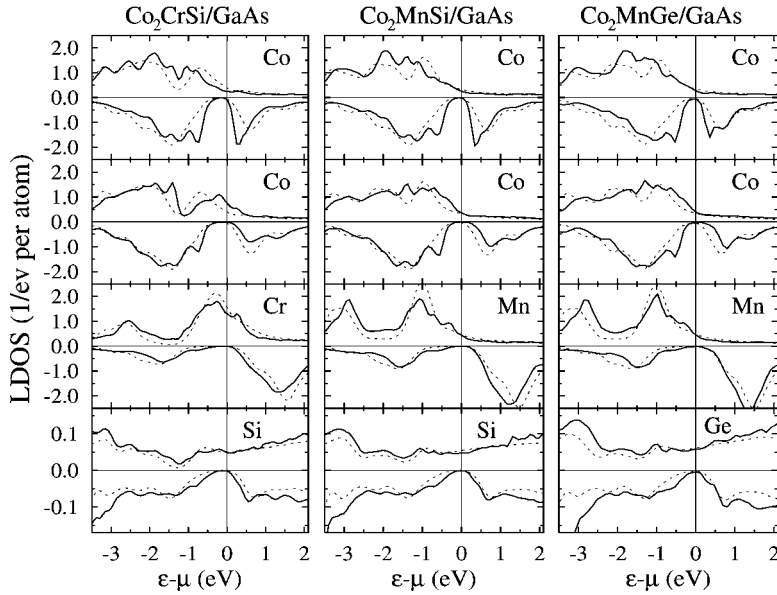


FIG. 6. LDOS at the  $\text{Co}_2\text{CrSi}/\text{GaAs}$ ,  $\text{Co}_2\text{MnSi}/\text{GaAs}$ , and  $\text{Co}_2\text{MnGe}/\text{GaAs}$  interfaces. The interfacial structures are set to (110)  $\text{CoZ-AsGa}$  ( $Z=\text{Si, Ge}$ ). The minority-spin LDOS is shown with negative sign. For comparison, the bulk LDOS is also presented as a dashed line.

strictly). This result again suggests that the nearly-half-metallic character at the (110) interface is in large part due to the properties of the GaAs (110) plane. Certainly, there also exist differences between these three alloys and  $\text{Co}_2\text{CrAl}$ . One is that the (110)  $\text{CoZ-AsGa}$  interface is not the most stable (110) interface for the three alloys while (110)  $\text{CoAl-AsGa}$  is so for  $\text{Co}_2\text{CrAl}$ . The other is that the three alloys do not lead to high spin polarization at the (110)  $\text{CoY-AsGa}$  interface while  $\text{Co}_2\text{CrAl}$  does at the (110)  $\text{CoCr-AsGa}$  interface. Though there appear such differences, it is still remarkable that a similar half-metal-like property is observed independently of the composition of the alloys as long as a specific interfacial structure is retained. It is also worth mentioning that for each of the three alloys, nearly-half-metallic (110)  $\text{CoZ-AsGa}$  is the second most stable, and the energy difference with respect to the most stable (110) interface, which is the  $\text{CoZ-GaAs}$  type, is just about  $0.1 \text{ J/m}^2$ . Thus, controlling the growth conditions (chemical potentials, pressure, etc.) may lead to stabilization of the (110)  $\text{CoZ-AsGa}$  interface, which is nearly half-metallic.

#### IV. CONCLUSIONS

In summary, we have investigated the electronic and structural properties of  $\text{Co}_2\text{CrAl}/\text{GaAs}$  interfaces using first-

principles calculations. Our results have shown that extremely high spin polarization is expected at the (110) interface although it is not the case for the (100) interface. The high spin polarization at the (110) interface remains almost invariant even if localized  $d$  components are eliminated from the LDOS, and this suggests that nearly-half-metallic character may be well reflected in transport properties. Furthermore, the analysis of adhesive strength predicts the stability of the nearly-half-metallic interfacial structure. Since high spin polarization is found also for  $\text{Co}_2\text{CrSi}/\text{GaAs}$ ,  $\text{Co}_2\text{MnSi}/\text{GaAs}$ , and  $\text{Co}_2\text{MnGe}/\text{GaAs}$  (110) interfaces, the discussion presented in this paper may be pertinent to other half-metallic alloys. All these findings suggest that (110) interfaces between half-metallic full Heusler alloys and GaAs (and possibly other III-V semiconductors) are worth further investigation.

#### ACKNOWLEDGMENTS

We thank K. Inomata for valuable discussions. This work was supported in part by a Grant-in-Aid for Scientific Research from the MEXT (Grant Nos. 14076105, 14076214, 16740162, 17064001, and 16310081) and also by the IT-program of Research Revolution 2002 from the MEXT.

- <sup>1</sup>R. A. de Groot, F. M. Mueller, P. G. van Engen, and K. H.J. Buschow, *Phys. Rev. Lett.* **50**, 2024 (1983).
- <sup>2</sup>A. Yanase and K. Siratori, *J. Phys. Soc. Jpn.* **53**, 312 (1984).
- <sup>3</sup>K. Schwarz, *J. Phys. F: Met. Phys.* **16**, L211 (1986).
- <sup>4</sup>W. E. Pickett and D. J. Singh, *Phys. Rev. B* **53**, 1146 (1996).
- <sup>5</sup>W. Pickett, *Phys. World* **11**, 22 (1998).
- <sup>6</sup>I. Galanakis, S. Ostanin, M. Alouani, H. Dreysse, and J. M. Wills, *Phys. Rev. B* **61**, 4093 (2000).
- <sup>7</sup>H. Akinaga, T. Manago, and M. Shirai, *Jpn. J. Appl. Phys., Part 2*

**39**, L1118 (2000).

- <sup>8</sup>W.-H. Xie, B.-G. Liu, and D. G. Pettifor, *Phys. Rev. B* **68**, 134407 (2003).
- <sup>9</sup>M. Bowen, M. Bibes, A. Barthélémy, J.-P. Contour, A. Anane, Y. Lematre, and A. Fert, *Appl. Phys. Lett.* **82**, 233 (2003).
- <sup>10</sup>M. Jullière, *Phys. Lett.* **54**, 225 (1975).
- <sup>11</sup>S. Picozzi, A. Continenza, and A. J. Freeman, *J. Appl. Phys.* **94**, 4723 (2003); *IEEE Trans. Magn.* **38**, 2895 (2002).
- <sup>12</sup>I. Galanakis, *J. Phys.: Condens. Matter* **16**, 8007 (2004).

- <sup>13</sup>I. Galanakis, M. Lezaić, G. Bihlmayer, and S. Blügel, *Phys. Rev. B* **71**, 214431 (2005).
- <sup>14</sup>G. A. de Wijs, and R. A. de Groot, *Phys. Rev. B* **64**, 020402(R) (2001).
- <sup>15</sup>P. Mavropoulos, I. Galanakis, and P. H. Dederichs, *J. Phys.: Condens. Matter* **16**, 4261 (2004).
- <sup>16</sup>K. Nagao, M. Shirai, and Y. Miura, *J. Appl. Phys.* **95**, 6518 (2004).
- <sup>17</sup>X.-G. Zhang, W. H. Butler, and A. Bandyopadhyay, *Phys. Rev. B* **68**, 092402 (2003).
- <sup>18</sup>S. S. P. Parkin, C. Kaiser, A. Panchula, P. M. Rice, B. Hughes, M. Samant, and S.-H. Yang, *Nat. Mater.* **3**, 862 (2004).
- <sup>19</sup>S. Yuasa, T. Nagahama, A. Fukushima, Y. Suzuki, and K. Ando, *Nat. Mater.* **3**, 868 (2004); K. Miyokawa *et al.*, *Jpn. J. Appl. Phys., Part 2* **44**, L9 (2004); S. Yuasa, A. Fukushima, T. Nagahama, K. Ando, and Y. Suzuki, *ibid.* **43**, L588 (2004).
- <sup>20</sup>K. Nagao, M. Shirai, and Y. Miura, *J. Phys.: Condens. Matter* **16**, S5725 (2004).
- <sup>21</sup>K. H. J. Buschow, and van P. G. Engen, *J. Magn. Magn. Mater.* **25**, 90 (1981).
- <sup>22</sup>Y. Miura, K. Nagao, and M. Shirai, *Phys. Rev. B* **69**, 144413 (2004); Y. Miura, M. Shirai, and K. Nagao, *J. Appl. Phys.* **95**, 7225 (2004).
- <sup>23</sup>H. J. Elmers, G. H. Fecher, D. Valdaitsev, S. A. Nepijko, A. Gloskovskii, G. Jakob, G. Schönhense, S. Wurmehl, T. Block, C. Felser, P.-C. Hsu, W.-L. Tsai, and S. Cramm, *Phys. Rev. B* **67**, 104412 (2003).
- <sup>24</sup>V. N. Antonov, H. A. Dur, Yu. Kucherenko, L. V. Bekenov, and A. N. Yaresko, *Phys. Rev. B* **72**, 054441 (2005).
- <sup>25</sup>K. Inomata, N. Tezuka, S. Okamura, H. Kurebayashi, and A. Hirohata, *J. Appl. Phys.* **95**, 7234 (2004).
- <sup>26</sup>K. Inomata, S. Okamura, R. Goto, and N. Tezuka, *Jpn. J. Appl. Phys., Part 2* **42**, L419 (2003).
- <sup>27</sup>J. P. Perdew, in *Electronic Structure of Solids '91*, edited by P. Ziesche and H. Eschrig (Akademie Verlag, Berlin, 1991), p. 11.
- <sup>28</sup>P. E. Blöchl, *Phys. Rev. B* **50**, 17953 (1994).
- <sup>29</sup>G. Kresse and D. Joubert, *Phys. Rev. B* **59**, 1758 (1999).
- <sup>30</sup>G. Kresse and J. Hafner, *Phys. Rev. B* **47**, R558 (1993); G. Kresse and J. Hafner, *Phys. Rev. B* **49**, 14251 (1994).
- <sup>31</sup>G. Kresse and J. Furthmüller, *Comput. Mater. Sci.* **6**, 15 (1996).
- <sup>32</sup>G. Kresse, and J. Furthmüller, *Phys. Rev. B* **54**, 11169 (1996).
- <sup>33</sup>Since the lattice parameter  $c$  is  $\sim 34$  Å for the (100) interface and  $\sim 36$  Å for the (110) interface, the  $10 \times 10 \times 1$   $\mathbf{k}$ -point grid leads to a little coarse sampling along the  $k_z$  direction in comparison with those along  $k_x$  and  $k_y$  directions. Therefore, we have tried  $10 \times 10 \times 2$   $\mathbf{k}$ -point grid for several interfaces and have confirmed that no significant change is observed for the optimized structures. In fact, the change of the force acting on each atom by the increase of the  $\mathbf{k}$ -point number is found to be less than  $0.1$  eV/Å.
- <sup>34</sup>I. Galanakis, *J. Phys.: Condens. Matter* **14**, 6329 (2002).
- <sup>35</sup>S. Picozzi, A. Continenza, G. Satta, S. Massidda, and A. J. Freeman, *Phys. Rev. B* **61**, 16736 (2000).
- <sup>36</sup>I. I. Mazin, *Phys. Rev. Lett.* **83**, 1427 (1999).
- <sup>37</sup>J. Hoekstra and M. Kohyama, *Phys. Rev. B* **57**, 2334 (1998).
- <sup>38</sup>I. G. Batirev, A. Alavi, M. W. Finnis, and T. Deutsch, *Phys. Rev. Lett.* **82**, 1510 (1999).
- <sup>39</sup>A. R. Lubinsky, C. B. Duke, B. W. Lee, and P. Mark, *Phys. Rev. Lett.* **36**, 1058 (1976).
- <sup>40</sup>See, for example, W. Mönch, *Semiconductor Surfaces and Interfaces* (Springer, Berlin, 1993).
- <sup>41</sup>V. Heine, *Phys. Rev.* **138**, A1689 (1965).